PV INTEGRATED SHIPBOARD MVDC GRID WITH REDUCED BUS VOLTAGE RIPPLE

Remna Radhakrishnan[1*] – Mariamma Chacko[2]

[1]Research Scholar, Department of Ship Technology, Cochin University of Science and Technology, Kerala, India
[2]Professor, Department of Ship Technology, Cochin University of Science and Technology, Kerala, India

ARTICLE INFO

***Article history*:**
Received: 17.01.2024.
Received in revised form: 23.04.2024.
Accepted: 25.07.2024.

Keywords:
Photovoltaic system
Onboard ship
Decarbonisation
Greenhouse gas emission
Bus voltage ripple
Shunt DC electric spring
Medium voltage DC grid.

DOI: https://doi.org/10.30765/er.2447

Abstract:

Integration of renewable energy sources for power generation is a proven solution to reduce the increasing greenhouse gas emissions towards decarbonisation onboard ships. Also, it is easy to integrate a variety of energy sources in an all-electric ship under medium voltage direct current distribution system. In such distribution system, high frequency switching power converters are greatly involved on the source and the load sides, which are massive source of harmonics. In this paper, a grid connected photovoltaic module is designed and paralleled with the generator, as a step towards reducing greenhouse gas emissions. Additionally, to take care of the voltage ripple and noise created by the high frequency switching power converters in the system, a shunt direct current electric spring with a control strategy is incorporated. The proposed system eliminates the use of heavy passive filters, commonly used at the rectifier end. MATLAB/Simulink results substantiate that the increased voltage ripple with the inclusion of energy sources and loads, that goes around 10.91% under fully loaded condition, is reduced to 1.27% with the shunt direct current electric spring, hence well within the IEEE 1709 std., which is less than 5%.

1. Introduction

In the scenario of increasing greenhouse gas (GHG) emissions onboard ships, the International Maritime Organisation (IMO) has already adopted certain strategies to reach, net zero GHG emissions close to the year 2050. Nowadays, the Maritime sector is behind 2.8% of GHG emissions [1], because of its rapid growth, dependence on carbon-intensive bunkers, and the sheer size of business. One of the three fundamental aspects put forward in the roadmap towards decarbonisation in the maritime industry [2] is technology development, specifically replacing the use of fossil fuels with others of renewable origin. Aiming at zero emissions in shipping and reducing the dependency on fossil fuels, the technical feasibility of a hybrid propulsion system merging green hydrogen with wind and solar energy is assessed in [3].

Solar energy utilization optimizes the ship design and reduces GHG emissions. In 2009, the IMO developed the Energy Efficiency Design Index (EEDI) to reduce GHG emissions from ships. The utilization of solar energy as an auxiliary power source was found to be an effective method to meet the IMO EEDI requirement [4]. A large-scale photovoltaic (PV) system-based ship's illumination system was developed in [5] for an onboard alternating current (AC) distribution system, with the help of batteries and a bidirectional converter operating under maximum power point tracking (MPPT).

An energy management system was developed [6] for ships having mixed energy sources including renewable energy source (RES), battery storage, shore power, marine fuels, etc. To preserve privacy and to achieve resilient and cost-effective operation of the islanded ship microgrid system [7], an energy management strategy was proposed. Topology design, stability analysis of large amounts of electronics components interaction, absence of standards for integrated design guiding practical projects, etc. are the major technical

* Corresponding author:
E-mail address: remna@cusat.ac.in.

challenges pointed out [8] for integrating distributed PV power into the medium voltage direct current (MVDC) grid. A soft-switched modular direct current (DC)-DC converter [9] was designed and developed for integrating wind/solar energy systems with MVDC transmission systems.

Apart from the tremendous advantages [10] in the MVDC onboard distribution system; increase in power electronic loads in the ship power system, increasing number of high-power pulsed loads (PPL), easy integration of RESs as a method for decarbonisation, etc., are some other reasons for the researchers to move towards MVDC distribution. Also, DC distribution systems do not have any frequency issues, but there exists some voltage instability issues [11].

IEEE 1709 std. specifies some voltage-related standards on 1 to 35 kV MVDC onboard ship distribution systems [12]. According to this, affordable voltage tolerance is ±10% and the voltage ripple and noise should not exceed 5%. However, the MVDC system becomes more fragile as the number of converters connected to the system increases [13]. Series active filters [14, 15] and a feedback linearization control method for series active filters [16] are some sort of research works carried out in literature to reduce the voltage ripples from source side active rectifiers. Fast-response DC filters were designed to suppress the low-frequency harmonics in the DC distribution network [17]. A model predictive controller was designed [18] to maintain the bus voltage stability in a small signal model of an MVDC ship power system containing a battery, energy storage system, propulsion motor (PM), and hotel loads which are connected through different power converters. To overcome the voltage instability issues in low-voltage DC grids, direct current electric springs (DCES) are being used nowadays and their operating principle, topology, applications, and control methods are summarised in [19]. Suppression of unbalanced voltage, improvement in power quality and voltage stability, DC bus voltage regulation, and harmonic cancellation [20] are the advantages of DCES. Basic modes of operation of shunt and series DCESs are narrated in [21]. In DC grids fed by RES, bidirectional buck-boost converter [22], full-bridge converter [23], and bidirectional DC-DC converter [24] are the topologies mainly used as series DCES. Commonly used shunt DCES topologies mentioned in literature are bidirectional buck-boost converter [25], bidirectional boost converter [26], and full-bridge converter [27]. Among shunt and series DCESs, [19] conclude that shunt DCES can remove harmonic currents without consuming extra energy.

Literature reveals that apart from GHG emission, voltage instability is also a major issue associated with shipboard DC distribution system. This paper recommends a solution for both these issues. In the aim of reducing the GHG emissions towards decarbonisation, a solar PV panel and an isolated boost converter is designed. Voltage instability issues in the system is addressed by the integration of a shunt DCES, with already proposed control strategy by the authors [28]. In addition to voltage stabilisation, this control strategy, inherently eliminates the use of passive inductor-capacitor (LC) filter that is usually used to eliminate the ripples after rectification.

The paper is organised as follows. Section 2 describes the system configuration and its major parts in detail. Simulation and results are explained in section 3, followed by conclusion.

2. System Configuration

In this section, details of the power generation and system loads of the ship's distribution system are explained. The system configuration given in Figure 1, details the major components of the system. All the sources and loads are connected to the bus through DC disconnect switches (DCDs).

The main power generation source in the system is a gas turbine-driven round-rotor synchronous generator. A solar PV panel is designed and connected on grid to assist decarbonisation, supports the power generation towards load demand. Propulsion motor (PM), DC service loads (DCSL), AC service loads (ACSL), and pulsed power loads (PPL) are the loads considered in the system. Inverters and isolated DC-DC converters are used for the conversion of the MVDC bus voltage into operating load voltages. PPLs are usually operated under offline mode (disconnected from the MVDC grid) with the aid of supercapacitors or flywheels. Here PPLs are accommodated online, keeping connected with the MVDC grid always, eliminating the presence of bulky supercapacitors and flywheels. The authors have already analysed the impact of the PPLs on bus voltage [29]. For making the bus voltage a low ripple one, in the presence of RES, a shunt DCES, with an already proposed control strategy is also connected across the MVDC bus. The passive LC filters that are usually used at the rectifier end are eliminated in this configuration, as the shunt DCES takes care of the high frequency harmonic injection from the rectifier to the DC bus.

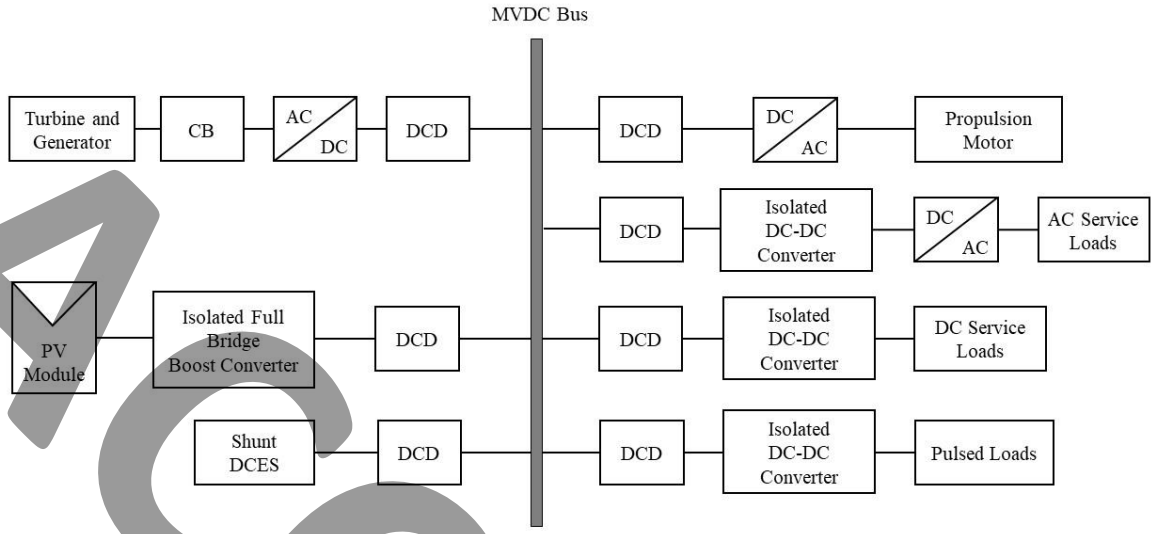

Figure 1 System configuration

2.1 Power Generator

A 30 MVA, 4160 V synchronous generator is the main power source in the system. An automatic voltage regulator (AVR) regulates its terminal voltage to the desired voltage level. An uncontrolled diode rectifier is used to convert the generated 4160 V AC into 5.7 kV DC. An in-built MATLAB/Simulink model of the generator and rectifier is used in this work. Specifications of the generator are given in Table 1.

2.2 PV Module

A PV module consists of a series connected group of solar cells called strings to build the driving force and these strings in parallel to supply the required current. PV panels used in marine vessels must be able to withstand environmental conditions like wind, humidity, shading and corrosion [30]. Specifications of the solar panel used for simulation is detailed in Table 1. A single solar panel is modelled using 60 series connected cells per string and 10 parallel connected strings. To limit the number of elements and to improve the simulation performance, voltage-controlled voltage source and current controlled-current source are used to scale the panel output voltage and current. Thus, PV module is modelled to generate a maximum of 880 kW under standard test conditions (STC), i.e., at a temperature of 25^0C and an irradiance of 1000 W/m^2. Assuming an average power of 300 kW, it can supply 3000 kWh per day. The voltage-current (V_{PV}-I_{PV}) and voltage-solar power (I_{PV}-P_{PV}) characteristics of the PV module are represented in Figure 2a and Figure 2b respectively.

PV panel output voltage is then boosted with the help of an isolated full bridge boost converter [31] whose circuit and control are depicted in Figure 3a and Figure 3b respectively. Insulated gate bipolar junction transistors (IGBTs) are the power semiconductor switch used in this topology with filter capacitors, C_1-C_2 and the boost inductor, L. The maximum power point voltage, V_{MPP} of the PV module is obtained through the popular perturb and observe (P&O) algorithm [25], which helps to stabilize the current fluctuations due to the varying input sunlight to the solar panels. The error between V_{MPP} and the solar voltage, V_{PV}, are corrected using a proportional integral (PI) controller. Pulse width modulated (PWM) signals at a switching frequency of 10 kHz, generated from the output of PI controller is fed to the power semiconductor switches of the converter. Output of the converter is directly connected to the grid through DCD switches. Specifications of PV module and the isolated full bridge converter are detailed in Table 1.

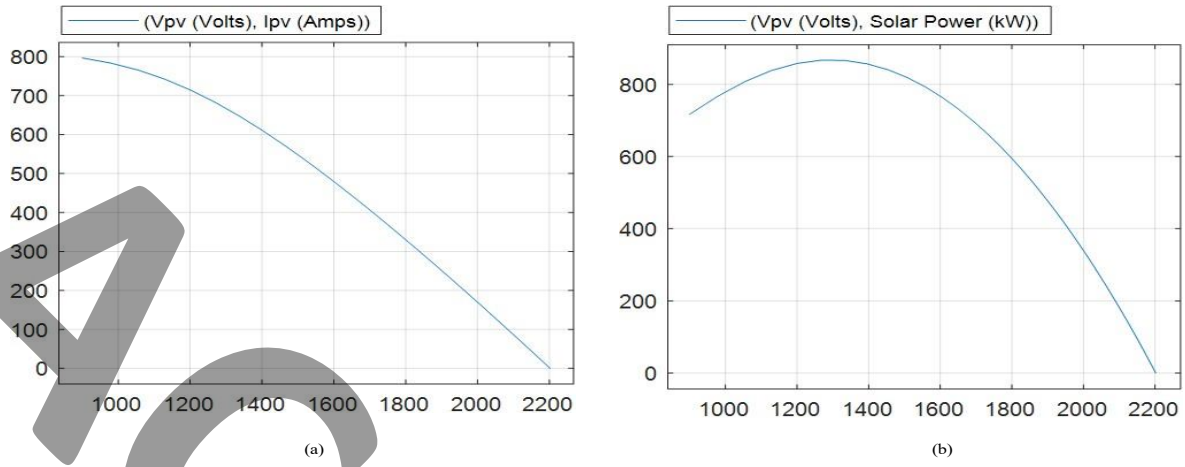

Figure 2 (a) Vpv-Ipv Characteristics (b) Vpv-Ppv Characteristics of PV module at STC

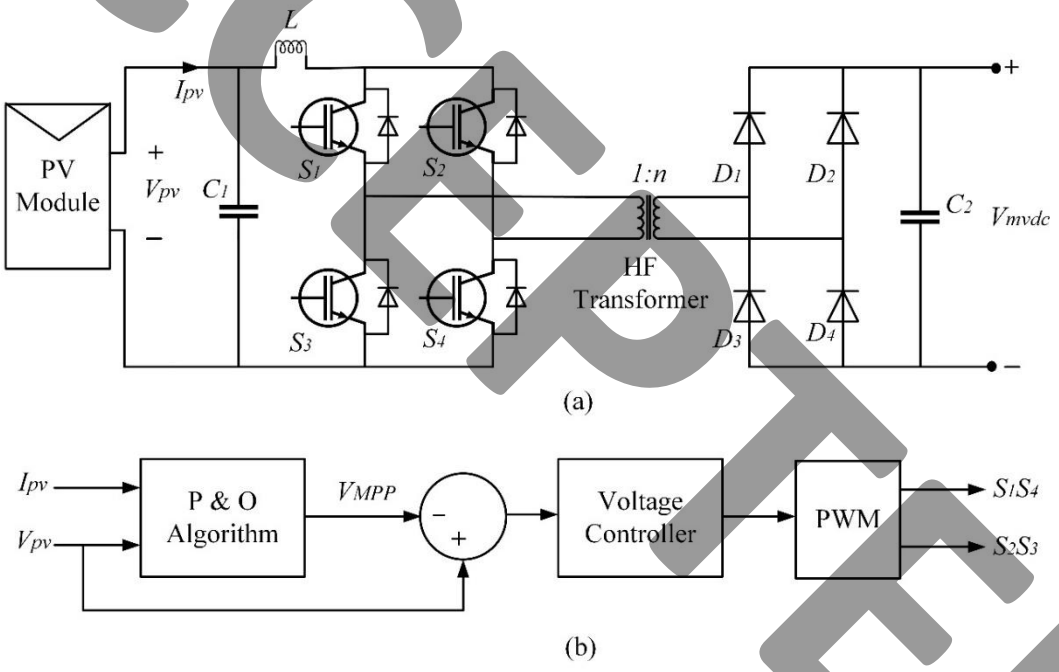

Figure 3 (a) Isolated Full Bridge Boost Converter (b) Control Circuit

2.3 System Loads

One of the most important system loads in AES, i.e., PM itself is the highest power-consuming load considered in this work. Induction motor (IM) is served as PM. Since the sustained speed range of naval ships is 40-70 knots, PM is designed to run corresponding to this at 100 rpm. A three-phase inverter drives the PM to follow the load torque profile, through the direct torque control (DTC) method.

The other set of loads considered in this work, DCSLs, ACSLs, and PPLs are supplied through isolated DC-DC converters. They are designed to operate at different voltage levels, like DCSLs at 220 V DC, ACSLs at 440 V AC, and PPLs at 3 kV DC. Three separate isolated DC-DC converters are designed to supply these voltages. For ACSLs, DC-AC converter is also used for voltage conversion. The topology of the isolated DC-DC converter using IGBTs is depicted in Figure 4. The inductor L in Figure 4, replicate the leakage inductance of the transformer primary winding, whereas *C1* and *C2* are the filter capacitors. Transformer turns ratios and the switching frequency of the converters are detailed in Table1. The output capacitor voltage is controlled by

regulating the maximum primary winding current of the high-frequency isolation transformer [32]. PWM switching signals for the IGBTs are generated based on this at a switching frequency of 10 kHz.

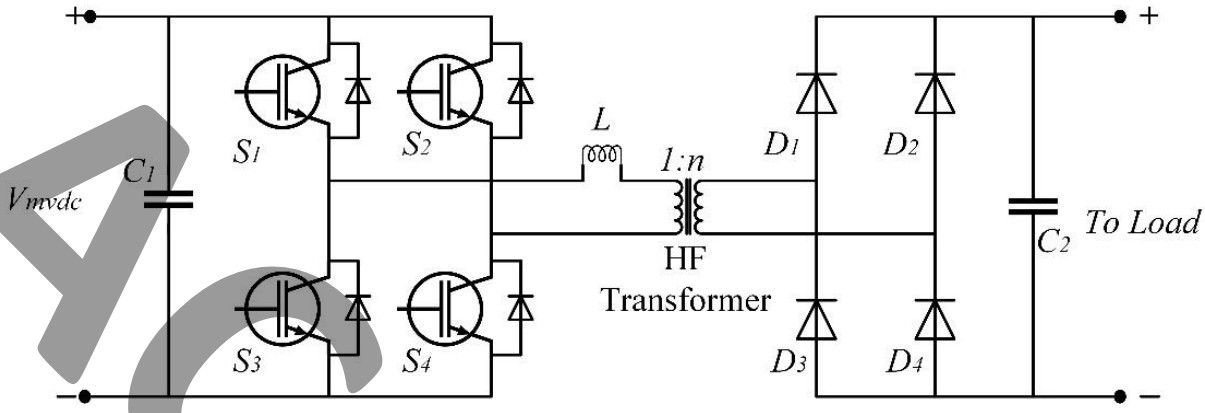

Figure 4 Isolated DC-DC Converter

2.4 Shunt DCES

As per IEEE 1709, the allowable bus voltage ripple onboard ship MVDC distribution system is limited to 5%. The presence of high-frequency switching converters both at the source and load sides, inject harmonics into the MVDC bus. These harmonics are the main reason for bus voltage ripple and noise. To bring the voltage ripple within the limits, a shunt DCES has been designed by the authors [28], whose topology using IGBTs is given in Figure 5a. The control law of shunt DCES is developed based on Equations 1 and 2. The switching signals generated based on the control circuit given in Figure 5b, decides the mode of operation of the shunt DCES, whether boosting discharging (BD) mode, suppressing charging (SC) mode or isolation mode.

$$V_{L\,dces} = -2V_{mvdc}D + (V_{mvdc} + V_{bat}) \quad (1)$$

$$I_{C\,dces} = I_{L\,dces} - I_{dces} \quad (2)$$

Where, $V_{L\,dces}$ – Voltage across L_{dces}

V_{mvdc} – MVDC bus Voltage

D –Duty ratio

V_{bat}– Battery voltage

$I_{C\,dces}$– Current through C_{dces}

$I_{L\,dces}$– Current through L_{dces}

I_{dces}– Shunt DCES current

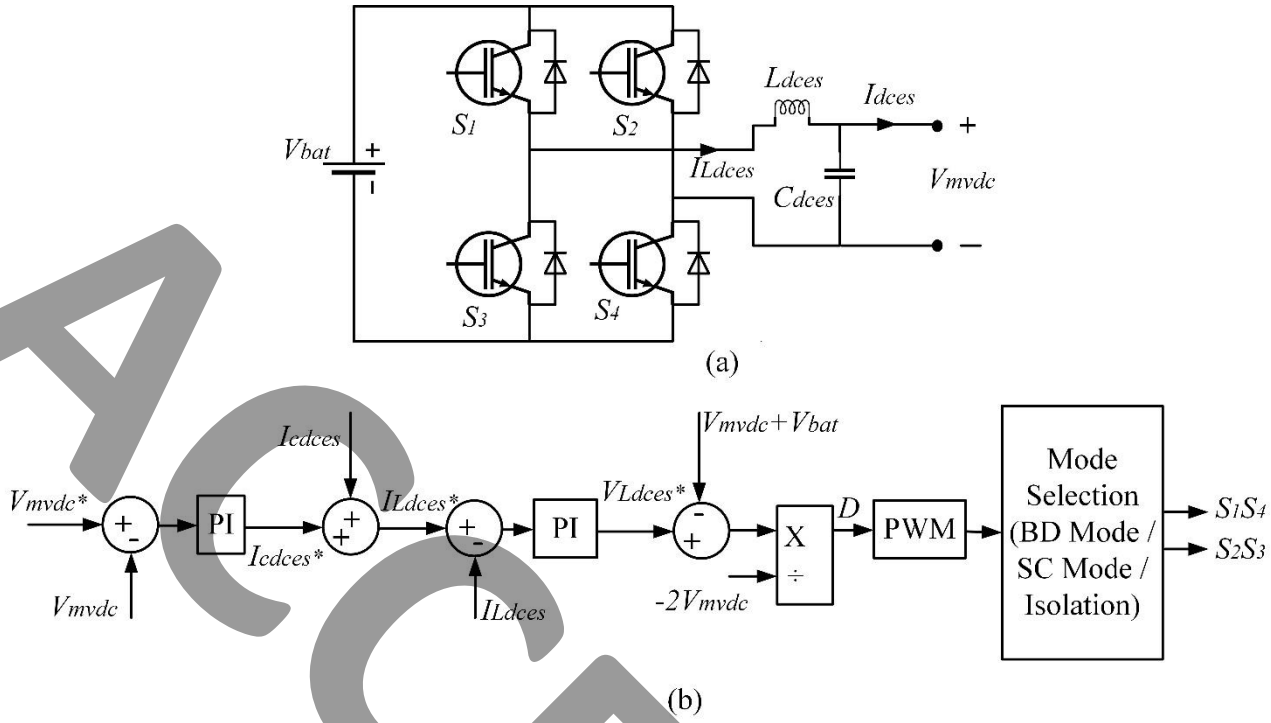

Figure 5 (a) Shunt DCES Topology (b) Control Circuit

Table 1: Specifications of the Components

Sl. No	Item	Rating
1	Generator	30 MVA, 4160 V, 2 pole, 60 Hz
2	PV Module	Manufacturer: Amerisolar, ThinFilm Dimension: 1408 X 1108 mm Short circuit current of a single solar cell= 0.82 A Open circuit voltage of a single solar cell= 0.62 V V_{pv}= 2200 V, I_{pv}= 400 A
3	Isolated Full Bridge Converter	f_{sw}=10 kHz, n=2.5
3	Shunt DCES	Battery capacity= 100Ahr, 5700V, f_{sw}=10 kHz
3	Propulsion Motor	19 MW, 4160 V, 12 pole, 60 Hz
4	ACSLs	7 MW, 440 V
5	DCSLs	360 kW, 220 V
6	PPL	4 MW, 3000 V
7	Isolated DC-DC Converter	f_{sw}=10 kHz, n_{PPL}=0.5, n_{ACSL}=0.07, n_{DCSL}=0.04

3. Simulation Results & Discussion

This section discusses the results obtained through the simulation. The system described in Figure 1 is simulated in MATLAB/Simulink using the Simscape toolbox. Specifications of the components [4, 33, 34, 35] used for simulation studies are detailed in Table 1. MATLAB/Simulink model is given in Figure 6.

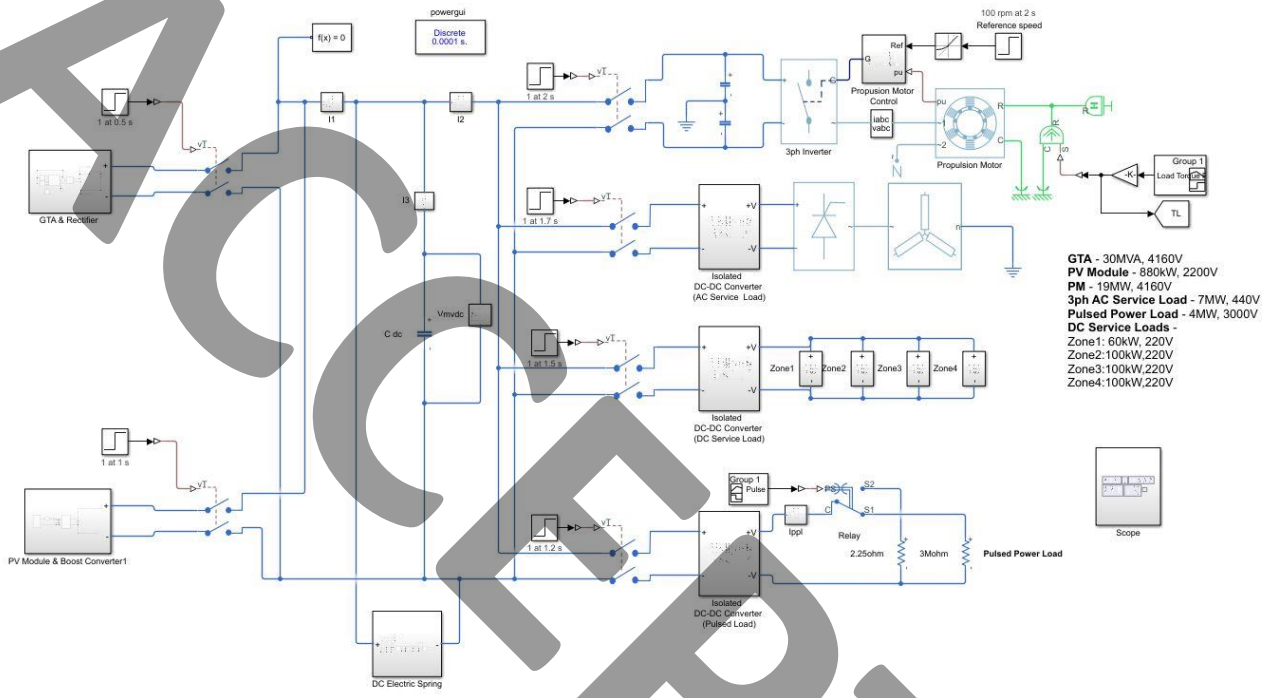

Figure 6 MATLAB/Simulink model of the System

Simulation is started by running the generator under no load. At 0.5 sec, DCD switch connected to the rectifier is closed and an average voltage of around 5868 V appears across the MVDC bus. Figure 7 depicts the MVDC bus voltage obtained by simulating the system described in Figure 1.

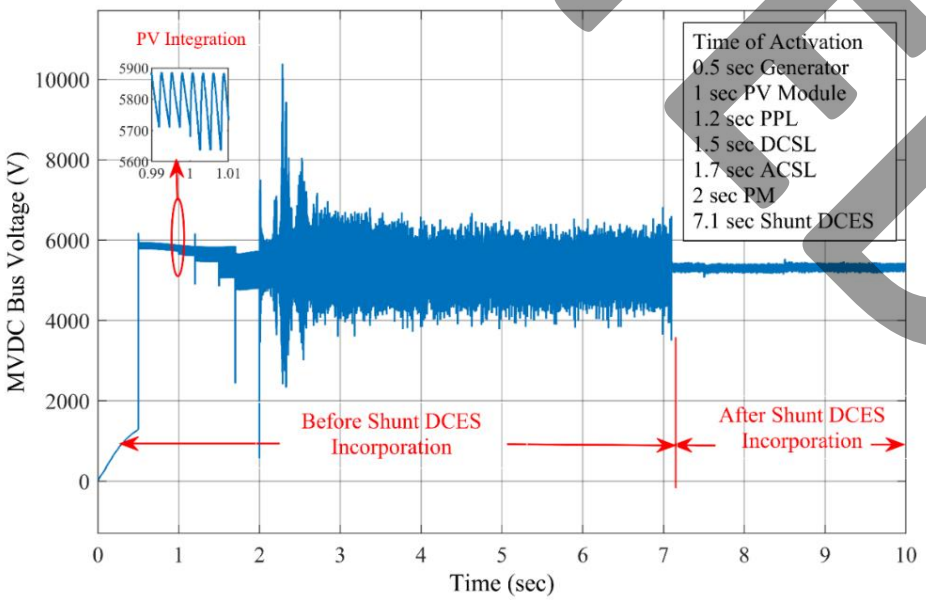

Figure 7 MVDC Bus Voltage

PV module is connected to the MVDC bus at 1 sec by closing the corresponding DCD switch. PV module is integrated at the aim of reducing the GHG emissions, but the associated boost converter injects harmonics to the MVDC bus, increasing the voltage ripple which is highlighted in Figure 7. Successively, the loads are activated one by one in the order of PPL, DCSL, ACSL, and PM at 1.2th, 1.5th, 1.7^{th,} and 2nd instants of simulation respectively. During the activation of these loads, there appears a transient dip/rise in bus voltage with an increase in ripple at each instant. Finally at 7.1th sec, shunt DCES is connected to the MVDC bus by closing the respective DCD switch. The voltage ripple, before and after the incorporation of shunt DCES can be clearly visualised in Figure 7.

Load side isolated DC-DC converters' output voltages for ACSLs, DCSLs, and PPLs are demonstrated in Figure. 8a, Figure 8b, and Figure. 8c respectively. The pulsating current flowing through the PPL load is shown in Figure 8c along with the PPL voltage. To visualise the change in PPL voltage ripple and current, one pulse is forced to flow before and one after the shunt DCES incorporation. The first current pulse, during the interval 5-6 sec creates noticeable ripple in PPL voltage and current as marked in Figure 8c. The second current pulse, during 7.5-8.5 sec, after shunt DCES incorporation, is smooth and free of ripple, compared to the previous current pulse. The impact of this current pulse on MVDC bus voltage is less significant, even under online PPL accommodation.

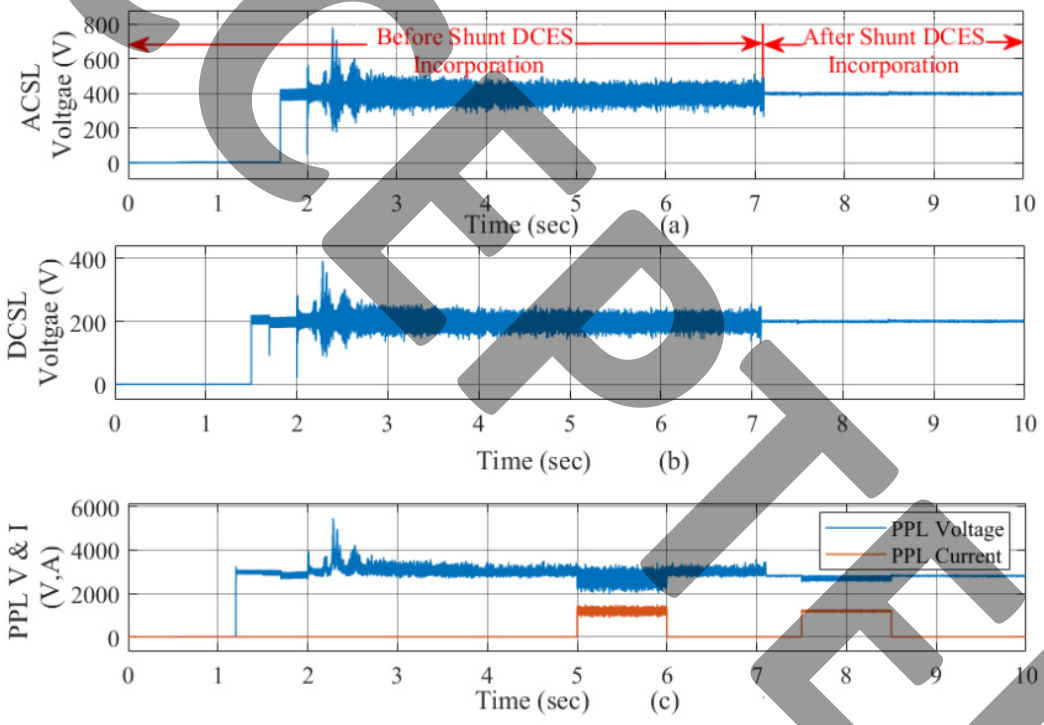

Figure 8 Load side DC Voltages of (a) ACSL, (b) DCSL, and (c) PPL Before and After Shunt DCES Incorporation

PM speed and torque waveforms are illustrated in Figure 9a and Figure 9b respectively. From the reference and actual speed of PM in Figure 9a, and the load torque and motor torque in Figure 9b, the DTC strategy is validated. The controller drives the motor at 100 rpm reference, for any load torque demand. The current drawn by the stator windings of the PM and the three-phase stator input phase voltages are marked in Figure 9c and Figure 9d respectively.

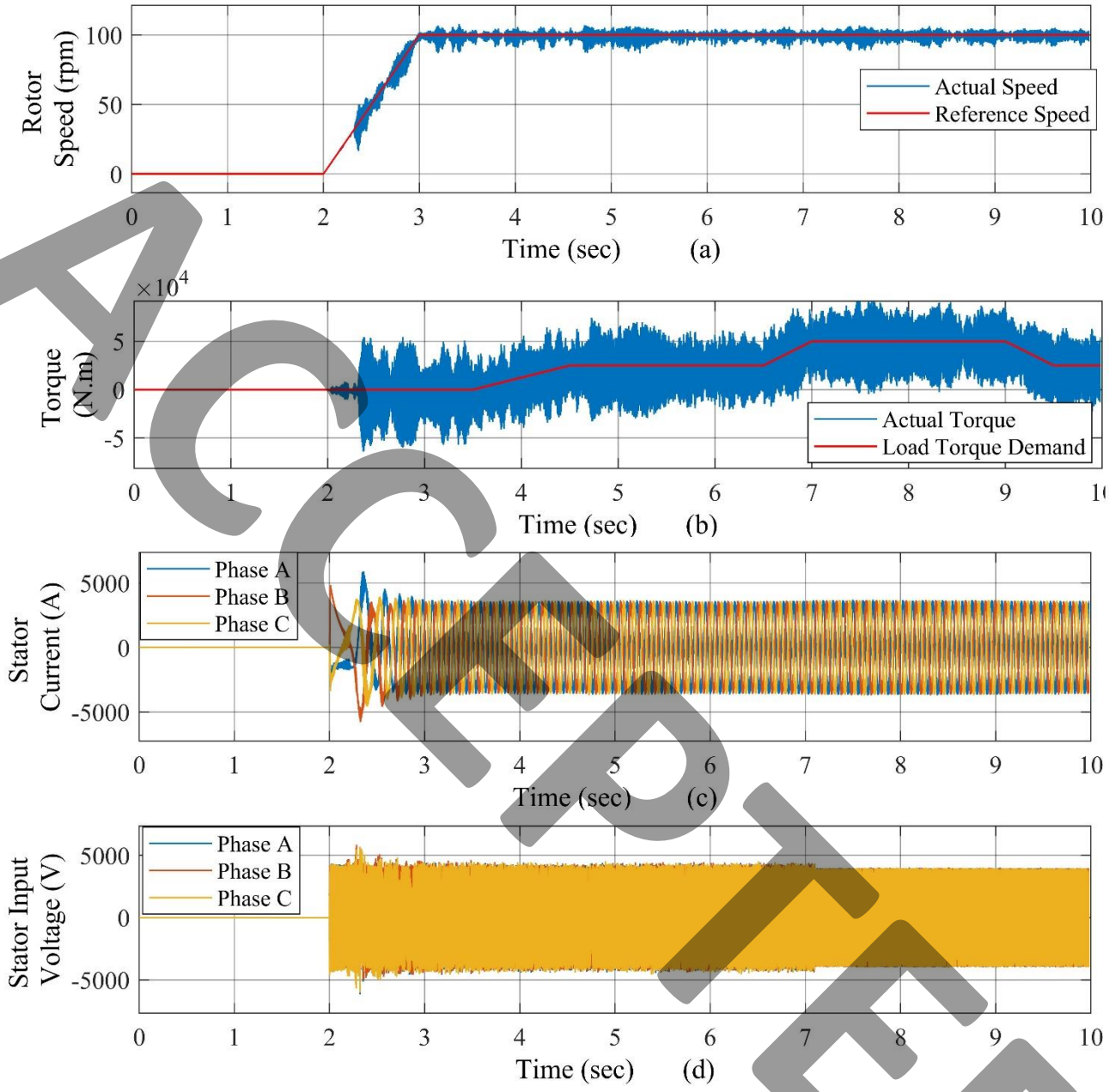

Figure 9 Propulsion Motor (a) Speed (b) Torque (c) Stator Current and (d) Stator Input Voltage

To show the increasing nature of voltage ripple in MVDC bus voltage and justify the operation of shunt DCES, both average MVDC bus voltage and total harmonic distortion (THD) with respect to DC value for 1cycle, during the instants, each source and load connected to MVDC bus are noted and tabulated in Table 2. The corresponding time intervals are noted in column 3. Also, the last row shows the THD with the incorporation of shunt DCES.

Table 2: Average Bus Voltage and THD

Sl. No	Connected Source/Load	Time Interval (Sec)	Average MVDC Bus Voltage (Volts)	THD (%)
1	Generator	0.51-0.526	5868	1.33
2	Generator & PV Module	1-1.016	5776	1.91
3	Generator, PV Module & PPL	1.2-1.216	5712	3.91
4	Generator, PV Module, PPL & DCSL	1.5-1.516	5563	6.44
5	Generator, PV Module, PPL, DCSL & ACSL	1.71-1.726	5278	7.65
6	Generator, PV Module, PPL, DCSL, ACSL & PM	5-5.016	5192	10.91
7	Generator, PV Module, PPL, DCSL, ACSL, PM & Shunt DCES	8-8.016	5297	1.27

Table 2 shows that the presence of harmonic contents in the MVDC bus voltage increases with the increase in number of loads connected to the MVDC bus. Starting from a THD value of 1.33%, due to the rectifier connected to the generator, it goes on increasing with the addition of PV module and each load, and reaches at a maximum of 10.91% under fully loaded condition. This THD value or the voltage ripple content is much above the IEEE 1709 recommended standard, which is less than 5%. From no load to peak load, the average bus voltage reduces from 5868 V to 5192 V. The last row shows that the integration of shunt DCES, have reduced the bus voltage THD to 1.27%, which is well within the IEEE 1709 std., with an increase in average bus voltage to 5297 V. For better understanding, THD plots before and after shunt DCES incorporation are demonstrated in Figure 10a and Figure 10b respectively. The results reveals that the shunt DCES could make the bus voltage ripple within the standards as per the IEEE 1709, i.e., below 5%. The simulation is carried out by taking the real system values from the references [4, 33, 34, 35], but the real ship electrical system is complex, having several nonlinear loads, power management and control. This is a limitation to the system simulation discussed in this paper, even then it helps in identifying the presence of harmonics in DC bus voltage and the shunt DCES incorporation will reduce the voltage ripple and noise at the DC bus.

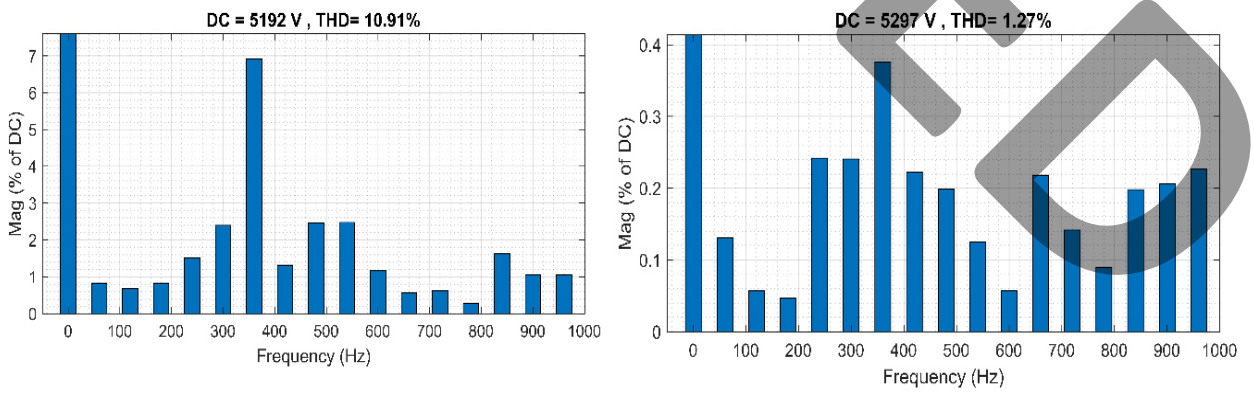

Figure 10 THD (a) Before Shunt DCES Incorporation (b) After Shunt DCES Incorporation

4. Conclusion

Technological advancements in power electronics gave rise to MVDC distribution onboard ships, with which the integration of different types of source and loads made easy. As a step towards decarbonisation, a grid connected PV module is integrated with the generator in this work. But the incorporation of RES and the associated boost converters along with other power converters deteriorated the MVDC bus voltage stability with an increased value of voltage ripple and noise. Shunt DCES integrated to the system is found to reduce the effect of these voltage harmonics, improving the stability of the system. MVDC bus voltage before and after this shunt DCES incorporation are analysed in this paper by plotting the THDs, and are found to be reduced to 1.27% from 10.91%, under fully loaded condition. This reduced voltage ripple, within the IEEE 1709 standard, i.e., less than 5% is achieved without the use of bulky passive LC filters. The paper thus puts forward a method for decarbonisation and voltage instability issues in the MVDC distribution system.

References

[1] J. e. a. Faber, "Fourth IMO GHG Study 2020 - Full report and annexes," 2020.

[2] E. Morante, "Roadmap to decarbonize the shipping sector: Technology development, consistent policies and investment in research, development and innovation," 2022.

[3] S. Dolatabadi, A. Ölçer and S. Vakili, "The Application of Hybrid Energy system (Hydrogen Fuel cell, wind, and solar) in shipping," *Renewable Energy Focus,* pp. 197-206, 2023.

[4] W. Zhu, J. Shi and S. Abdelwahed, "End-to-end system level modelling and simulation for medium-voltage DC electric ship power systems," *International Journal of Naval Architecture and Ocean Engineering,* pp. 37-47, 2018.

[5] R. Tang, "Large-Scale photovoltaic system on green ship and its MPPT controlling," *Solar Energy,* pp. 614-628, 2017.

[6] K. Yigit and B. Acarkan, "A new electrical energy management approach for ships using mixed energy sources to ensure sustainable port cities," *Sustainable Cities and Society,* pp. 126-135, 2018.

[7] K. Lai and M. Illindala, "A distributed energy management strategy for resilient shipboard power system," *Applied Energy,* pp. 821-832, 2018.

[8] C. Wei, Q. Li, Z. Wang, H. Liu and C. Liu, "Technical challenges of integrating high proportion distributed photovoltaic power into medium DC grid," in *8th Renewable Power Generation Conference (RPG 2019)*, Shanghai, China, 2019.

[9] E. Mathew and A. Das, "Integration of renewable energy sources with MVDC network," in *IEEE International Conference on Power Electronics, Drives and Energy Systems (PEDES)*, Jaipur, India, 2020.

[10] N. Doerry and J. Amy, "MVDC Distribution Systems," in *Conference: ASNE AMTS*, Philadelphia, 2018.

[11] S. Coffey, V. Timmers, R. Li, G. Wu and A. Egea-Alvarez, "Review of MVDC Applications, Technologies and Future Prospects," *Energies,* vol. 14, no. 24, p. 8294, 2021.

[12] I. S. 1.-2. (. o. I. S. 1.-2. 1709-2018, "IEEE Recommended Practice for 1 kV to 35 kV Medium-Voltage DC Power Systems on Ships," pp. 1-54, 2018.

[13] H. Huang, F. Liu and X. Zha, "Mechanism of Power Quality Deterioration Caused by Multiple Load Converters for the MVDC System," *Frontiers in Energy Research,* 2022.

[14] B. Engelhart and A. Bazzi, "Design and Control of a Series DC Active Filter (SDAF) for MVDC Marine Applications," in *IEEE Transportation Electrification Conference & Expo (ITEC)*, Chicago, IL, USA, 2020.

[15] H. Mirzaee, B. Parkhideh and S. Bhattacharya, "Design and control of Series DC Active Filter (SDAF) for shipboard Medium-Voltage DC power system," in *IEEE Electric Ship Technologies Symposium*, Alexandria, VA, USA, 2011.

[16] Y. Jeung, D. Lee and H. Lee, "Feedback linearization control of series active DC filters for MVDC shipboard power Systems," in *16th European Conference on Power Electronics and Applications*, Lappeenranta, Finland, 2014.

[17] J. Liao, N. Zhou and Q. Wang, "Design of Low-Ripple and Fast-Response DC Filters in DC Distribution Networks," *Energies,* 2018.

[18] A. Saad, S. Faddel, T. Youssef and O. Mohammed, "Small-signal model predictive control based resilient energy storage management strategy for all electric ship MVDC voltage stabilization," *Journal of Energy Storage,* pp. 370-382, 2019.

[19] M. Wang, K. T. Mok, S. C. Tan and S. Y. Hui, "Multifunctional DC Electric Springs for Improving Voltage Quality of DC Grids," *IEEE Transactions on Smart Grid,* pp. 2248-2258, 2018.

[20] H. C. C. S., S. B. and S. K.S., "Analysis of DC Electric Springs in the Micro Grid System Consisting of Fluctuating Energy Sources," *Energy Procedia,* pp. 114-123, 2016.

[21] D. Moeini, A. Chandra and A. Kaymanesh , "Application of DC Electric Spring in Modern DC Microgrids, Review and Proposition," in *IEEE Electrical Power and Energy Conference (EPEC)*, Toronto, ON, Canada, 2021.

[22] R. Hashem, Y. Soliman, S. Al-Sharm and A. Massoud, "Design of an electric spring for power quality improvement in PV-based DC grid," in *IEEE Symposium on Computer Applications & Industrial Electronics (ISCAIE)*, Penang, Malaysia, 2018.

[23] M. H. Wang, S. Yan, S. Tan, Z. Xu and S. Y. Hui, "Decentralized Control of DC Electric Springs for Storage Reduction in DC Microgrids," *IEEE Transactions on Power Electronics,* pp. 4634-4646, 2019.

[24] J. Zhang, Y. Wu, M. Liu and W. Ji, "Research on Application of DC Electric Spring in DC Distribution Network," in *The 10th Renewable Power Generation Conference (RPG 2021),Online Conference*, 2021.

[25] A. A. G., H. R. and U. S., "A Shunt DC Electric Spring-Based Control Strategy for Real-Time Critical and Noncritical Load Management in DC Microgrid," *International Transactions on Electrical Energy Systems,* 2022.

[26] X. Chen, M. Shi, H. Sun, Y. Li and H. He, "Distributed Cooperative Control and Stability Analysis of Multiple DC Electric Springs in a DC Microgrid," *IEEE Transactions on Industrial Electronics,* pp. 5611-5622, 2018.

[27] S. P. Gawande, A. R. Nagpure, K. Dhawad and P. Chaturvedi, "Characteristics Behavior of Shunt DC Electric Spring for Mitigating DC Microgrid Issues," in *IEEE First International Conference on Smart Technologies for Power, Energy and Control (STPEC)*, Nagpur, India, 2020.

[28] R. Radhakrishnan and M. Chacko , "A Shunt DC Electric Spring Control Strategy for MVDC Bus Voltage Stability Onboard AES," *Recent Advances in Electrical & Electronic Engineering,* 2023.

[29] R. Radhakrishnan and M. Chacko , "Impact of online PPL accommodation on quality of power in an AES' MVDC distribution system," *International Journal of Advanced Technology and Engineering Exploration,* pp. 1056-1072, 2022.

[30] T. Emmanuel and P. John, "PV Systems Installed in Marine Vessels: Technologies and Specifications," *Advances in Power Electronics,* 2013.

[31] L. R. De Oliveira, P. S. N. Filho, T. A. dos Santos Barros, M. G. Villalva and E. Ruppert, "nput voltage regulation of an isolated full-bridge boost converter fed by a photovoltaic device with the state-space feedback control method," in *Brazilian Power Electronics Conference*, Gramado, Brazil, 2013.

[32] H. Suryanarayana and . S. D. Sudhoff, "Average-value modelling of a peak-current controlled galvanically-isolated DC-DC converter for shipboard power distribution," in *IEEE Electric Ship Technologies Symposium (ESTS)*, Arlington, VA, USA, 2013.

[33] M. M. Marden, P. Prempraneerach, J. L. Kirtley, G. Karniadakis and C. Chryssostomidis, "An end-to-end simulator for the all-electric ship MVDC integrated power system," in *Conference on Grand Challenges in Modelling & Simulation (GCMS '10), Society for Modeling & Simulation International*, Vista, CA, 2010.

[34] L. Zhou, H. Liu and L. Bai, "Modeling and simulation of all-electric ships with medium-voltage DC integrated power system," in *IEEE Conference and Expo Transportation Electrification Asia-Pacific (ITEC Asia-Pacific)*, Beijing, 2014.

[35] J. Shi, R. Amgai and S. Abdelwahed, "Modelling of Shipboard medium-voltage direct current system for system level dynamic analysis," *IET Electrical System in Transportatio,* pp. 156-165, 2015.

[36] N. Doerry and . J. Amy, "The Road to MVDC, Article by Naval Sea Systems Command.," 2015.

[37] IMO, "Fourth IMO GHG Study," 2020.

[38] C. X., S. M., S. H., L. Y. and H. H., "Distributed Cooperative Control and Stability Analysis of Multiple DC Electric Springs in a DC Microgrid," *IEEE Transactions on Industrial Electronics,* pp. 5611-5622, 2018.